

Semiconductor disk laser with a wavelength of 780 nm based on a MOCVD-grown $\text{Al}_x\text{Ga}_{1-x}\text{As}/\text{Al}_y\text{Ga}_{1-y}\text{As}$ heterostructure with optical and electron beam pumping

M.R. Butaev, Ya.K. Skasyrsky, V.I. Kozlovsky, A.Yu. Andreev, I.V. Yarotskaya, A.A. Marmalyuk

Abstract. A pulsed semiconductor disk laser based on the $\text{Al}_x\text{Ga}_{1-x}\text{As}/\text{Al}_y\text{Ga}_{1-y}\text{As}$ structure with resonantly periodic gain and a built-in Bragg mirror emitting at a wavelength near 780 nm is studied. The laser characteristics are presented both for pumping by an electron beam and for optical pumping by laser diode radiation with a wavelength of 450 nm. Under pumping by an electron beam, a peak power of 4.4 W is achieved with a slope efficiency of over 10%, while under optical pumping, the power is 0.2 W with a slope efficiency of 2.2% and approximately the same cavity parameters. Possible reasons for the lower powers and efficiency under optical pumping are discussed.

Keywords: semiconductor disk laser, $\text{Al}_x\text{Ga}_{1-x}\text{As}/\text{Al}_y\text{Ga}_{1-y}\text{As}$ structure, quantum well, electron beam, optical pumping, MOCVD.

1. Introduction

High-power, wavelength-tunable laser sources with narrow emission lines are widely used in a number of scientific and industrial fields. In particular, they are necessary for the development of quantum technologies based on cold atoms with transitions at optical frequencies. These requirements are fully met by optically pumped semiconductor disk lasers (SDLs) [1]. For example, a laser with a wavelength near 689 nm and a linewidth of 125 Hz has been recently demonstrated for cooling Sr atoms [2]. The same paper also discusses the advantages of SDLs over other lasers used for these purposes, including small-size external-cavity laser diodes, which is due to the relatively low level of spontaneous noise and the absence of relaxation oscillations in SDLs.

In this work, we consider the possibility of fabricating a SDL with an emission wavelength near 780 nm. A laser in this range is needed to cool Rb atoms. Kahle et al. [3] have already demonstrated a SDL with a given wavelength. They used a relatively new scheme of a membrane-type SDL with an active heterostructure (grown by molecular beam epitaxy)

with several quantum wells (QWs) without a built-in Bragg mirror [3]. The technology of separating the heterostructure from the growth substrate and sandwiching it between two cold-conducting SiC plates was rather complicated. In this case, the cavity was formed by two external mirrors. Pumping was performed by a rather expensive Coherent Verdi-V18 laser with a wavelength of 532 nm, based on intracavity generation of the second harmonic of an optically pumped SDL.

The aim of this work was to develop and grow a heterostructure by metalorganic chemical vapour deposition (MOCVD) with a built-in Bragg mirror at a wavelength of 780 nm and to compare the characteristics of a SDL with optical laser diode pumping and a SDL with electron beam pumping. The relevance of pumping by an electron beam increases with the development of SDLs based on wide-gap heterostructures, for which there are practically no effective pump sources available.

2. Experiment

The heterostructure was grown by metal-organic vapour deposition and contained a built-in Bragg mirror of 30 pairs of $\text{Al}_{0.3}\text{Ga}_{0.7}\text{As}/\text{Al}_{0.9}\text{Ga}_{0.1}\text{As}$, ten 12-nm-thick $\text{Al}_{0.139}\text{Ga}_{0.861}\text{As}/\text{Al}_{0.3}\text{Ga}_{0.7}\text{As}$ QWs successively grown on an *n*-type GaAs substrate with an arrangement period corresponding to half the wavelength [$\lambda_0/2N(\lambda_0)$, where $\lambda_0 = 780$ nm and $N = 3.47$ is the average refractive index], and an $\text{Al}_{0.55}\text{Ga}_{0.45}\text{As}$ layer that plays the role of a barrier for carrier diffusion to the surface. The photoluminescence and reflectance spectra of the obtained structure are shown in Fig. 1. We believe that two intense peaks in the luminescence spec-

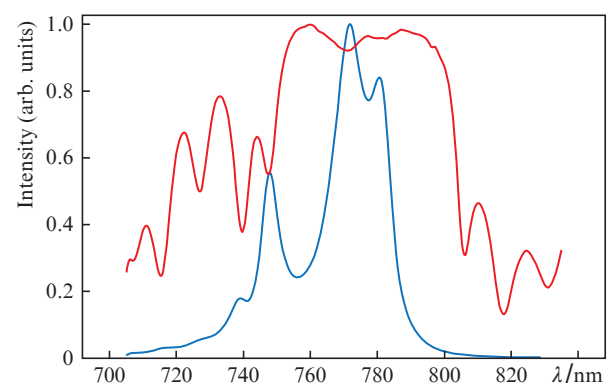


Figure 1. (Colour online) Photoluminescence (blue curve) and reflectance (red curve) spectra of the structure.

M.R. Butaev, V.I. Kozlovsky Lebedev Physical Institute, Russian Academy of Sciences, Leninsky prosp. 53, 119991 Moscow, Russia; National Research Nuclear University MEPhI, Kashirskoe sh. 31, 115409 Moscow, Russia; email: vikoz@sci.lebedev.ru;

Ya.K. Skasyrsky Lebedev Physical Institute, Russian Academy of Sciences, Leninsky prosp. 53, 119991 Moscow, Russia;

A.Yu. Andreev, I.V. Yarotskaya, A.A. Marmalyuk OJSC M.F. Stel'makh Polyus Research Institute, ul. Vvedenskogo 3, stroenie 1, 117342 Moscow, Russia

Received 23 December 2021

Kvantovaya Elektronika 52 (4) 362–366 (2022)

Translated by V.L. Derbov

trum with maxima at $\lambda = 772$ and 748 nm are due to radiative recombination of electrons and holes from the ground and first excited levels in the QW, respectively. Small peaks at $\lambda = 739$ and 780 nm can be attributed to the modes of a low- Q resonator formed by a Bragg mirror and the surface of the structure.

A schematic of the laser is presented in Fig. 2. In principle, it is similar in the cases of optical and electron-beam pumping. The structure is fixed on a copper cold plate with a temperature of approximately 20°C and is pumped by an electron beam from the side at an angle of 30° . The optical pumping is performed at an angle of 60° . A built-in Bragg mirror and an external concave spherical mirror with a radius of curvature of 30 mm form the cavity. The reflection coefficient of the outer mirror at a wavelength of 780 nm was 98% . The cavity length was 27 mm for electron-beam pumping and 29 mm for optical pumping. The scheme of radiation extraction from the vacuum chamber in the case of electron-beam pumping is described in more detail in Ref. [4].

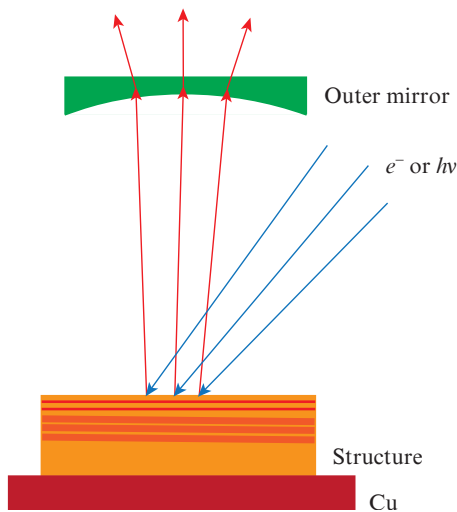


Figure 2. (Colour online) Schematic of a semiconductor disk laser.

When pumped by an electron beam, the maximum power was achieved using electrons with an energy of 30 keV and an excitation spot with a diameter approximately equal to the transverse size of the fundamental cavity mode $2w_0 = 65$ μm . The laser was aligned as follows. The electron beam was pulse-scanned at a frequency of 50 Hz along the line, which then slowly moved in the perpendicular direction until it intersected with the cavity mode. The pump duration was determined by the scanning rate and amounted approximately to 100 ns.

Optical pumping was performed by a commercial laser diode (LD) based on an InGaN/GaN heterostructure with a built-in focusing system. Using this system, the LD radiation was focused into a spot with a size of 70×70 μm . To start the LD in a pulsed regime, a self-made driver was used, which formed a pulse with a duration of ~ 200 ns. The LD radiation wavelength in the pulsed regime was 450 nm. The characteristics of the optically pumped laser were measured at a pulse repetition rate of 250 Hz; with its increase to 3 kHz, no significant change in the peak power was observed. The peak powers of the pump laser and SDL were measured with calibrated FEK-29 and FEK-22 coaxial photocells.

3. Experimental results

3.1. Electron-beam pumping

Figure 3 shows the dependence of the peak laser radiation power on the electron beam current.

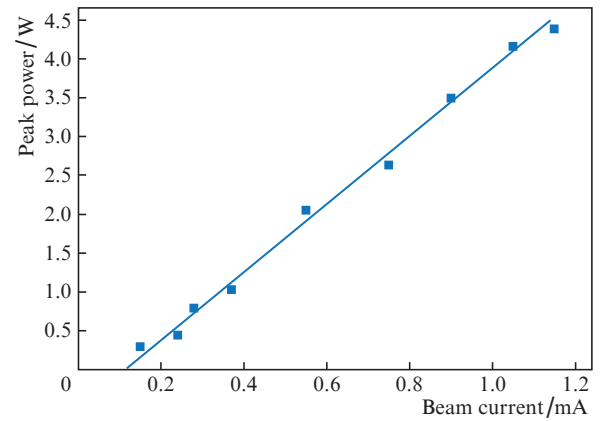


Figure 3. (Colour online) Dependence of the laser pulse power on the electron beam current.

At an electron beam current of 1.2 mA, the maximum output power was 4.4 W; the slope efficiency of the laser was 12% , and the oscillation threshold current was 0.1 mA, which for a spot diameter of 65 μm on the structure corresponds to the threshold current density of 3 A cm^{-2} or the beam intensity of 90 kW cm^{-2} . The oscillation threshold with respect to the pump power launched in the active region of the structure is noticeably lower, since approximately 25% of the electron beam energy is not supplied to the structure, but is carried away by reflected and secondary electrons, and approximately the same amount of energy remains in the electrons that fly through the active region of the structure without completely delivering their energy to it.

Figure 4 shows a typical oscillogram of a SDL oscillation pulse with a duration of 100 ns in the base. The duration and shape of the pulse depend on the scanning speed, the diameter of the electron beam spot, and the degree of alignment of the scan line with the position of the fundamental mode. As the

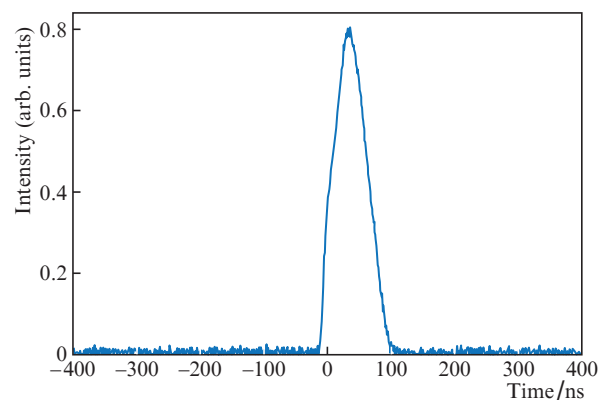


Figure 4. (Colour online) Oscillogram of the SDL oscillation pulse at an electron beam current of 1 mA.

scan rate decreases, the pulse duration can be increased, but the peak laser power decreases.

The SDL oscillation spectrum is shown in Fig. 5. One line with a maximum at $\lambda = 779.4$ nm and a FWHM of 1.4 nm is observed.

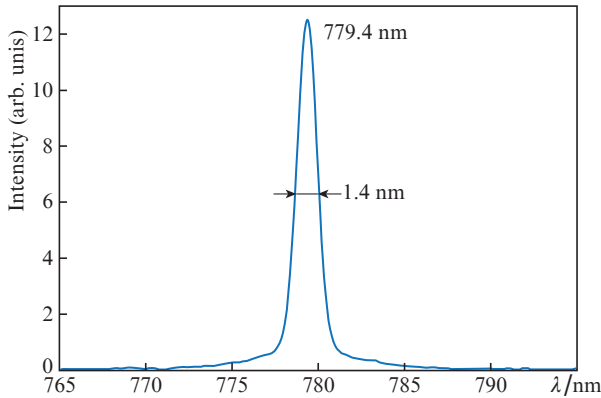


Figure 5. (Colour online) Spectrum of SDL oscillation at an electron beam current of 1 mA.

The pattern of the far-field radiation strongly depends on the alignment of the laser. Figure 6 shows examples of the distribution of the radiation field in the far-field zone. Near the threshold, the total divergence angle is ~ 10 mrad. It should be also noted that the outer mirror substrate is a diverging lens, which increases the divergence of the radiation coming out of a resonator close to semi-concentric by a factor of almost 1.5.



Figure 6. Radiation field patterns in the far-field zone at different laser alignments.

3.2. Optical pumping

Oscillograms of SDL oscillation pulses and LD pump radiation are shown in Fig. 7. The complex shape of the LD radiation pulse is due to the imperfection of the used driver. The FWHM duration of the oscillation pulse was 140 ns.

Figure 8 demonstrates the dependence of the peak power of oscillation on the peak power of the pump radiation, absorbed by the structure (the LD power minus the power reflected from the structure surface).

At a useful pump power of 11.5 W, the lasing power was ~ 0.2 W. The oscillation threshold was estimated as 2.6 W (68 kW cm^{-2}), and the slope efficiency was 2.2%. The achieved values of the power and efficiency of the laser are significantly inferior to those obtained by electron-beam pumping, although the limiting efficiency of a laser pumped by an electron beam has a physical limitation of $\sim 30\%$ [5].

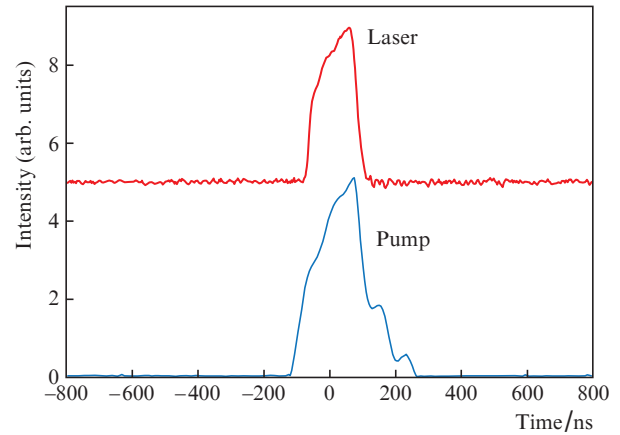


Figure 7. (Colour online) Oscillograms of SDL oscillation pulses and LD pump radiation.

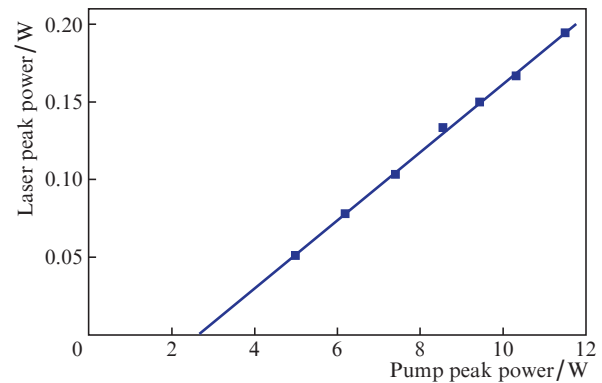


Figure 8. (Colour online) Dependence of the SDL peak power on the peak power of the pump radiation absorbed by the structure.

Figure 9 shows the SDL oscillation spectrum under optical pumping. The oscillation line maximum corresponds to $\lambda = 780.7$ nm, and the line width at half maximum is 1.2 nm. These values are close to those obtained upon pumping with an electron beam.

Figure 10 shows the pattern of the far field of SDL radiation under optical pumping. The radiation divergence at a

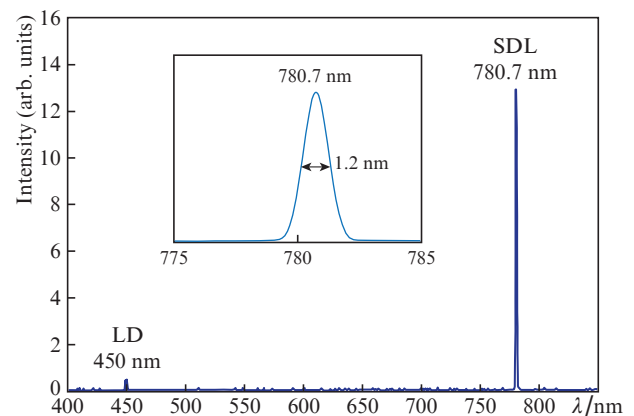


Figure 9. (Colour online) Spectrum of oscillation of SDL under optical pumping.

small excess of the threshold is somewhat larger than in Fig. 6, since the length of the resonator under optical pumping is closer to the radius of curvature of the external mirror, which leads to a decrease in the fundamental mode diameter.

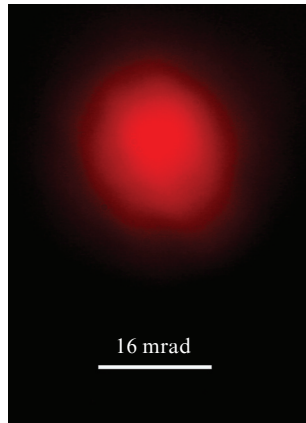


Figure 10. (Colour online) Pattern of the far field of SDL radiation under optical pumping.

4. Discussion of the results

An unexpected result of this work is the low efficiency of the laser under optical pumping. We assume that this is due to the energy band structure of the $\text{Al}_{0.3}\text{Ga}_{0.7}\text{As}$ barrier layers, in which the pump mainly generates nonequilibrium charge carriers. Unfortunately, we failed to find the energy band diagram of $\text{Al}_{0.3}\text{Ga}_{0.7}\text{As}$ in the literature. Figure 11a schematically shows the band diagram of $\text{Al}_x\text{Ga}_{1-x}\text{As}$ at $x < 0.4$, when the solid solution still remains direct-gap [6]. Three valleys form in the conduction band: Γ , X , and L . The corresponding energy gaps from the minima of these valleys to the top of the

valence band E_Γ , E_X , and E_L change with the composition of the solid solution in accordance with Fig. 11b [7].

It can be seen from Fig. 11 that upon absorption of radiation with $\lambda = 450$ nm (2.75 eV), direct transitions with the formation of electrons are possible not only in the Γ valley, but also in the X and L valleys. Moreover, the absorption coefficient for transitions in the X and L valleys is much higher, since the density of states in the valence band increases significantly with increasing wave vector.

Further, if $x < 0.4$, the nonequilibrium carriers from the side valleys quickly pass to the deep Γ valley due to intense electron–phonon scattering [8]. But even if $x > 0.45$, nonequilibrium electrons from the side valleys, falling into the $\text{Al}_{0.139}\text{Ga}_{0.861}\text{As}$ layer of the quantum well with a low content x , pass into the Γ valley of the QW [8]. Therefore, even in the case of using an indirect-gap $\text{Al}_{0.58}\text{Ga}_{0.42}\text{As}$ barrier layer, a fairly high oscillation efficiency was achieved in [3].

Nevertheless, the presence of direct transitions with the photoexcitation of nonequilibrium electrons to side valleys can lead to a deterioration in the laser characteristics due to the large absorption coefficient. According to [9], the absorption coefficient for $\text{Al}_{0.3}\text{Ga}_{0.7}\text{As}$ reaches $1.5 \times 10^5 \text{ cm}^{-1}$ at a pump wavelength of 450 nm. Such a high absorption coefficient leads to the fact that most of the pump energy is absorbed already in the first barrier layer, and most of the QWs remain weakly pumped, which leads to a deterioration in the lasing characteristics. For comparison, the absorption coefficient of radiation with a wavelength of 532 nm in the $\text{Al}_{0.58}\text{Ga}_{0.42}\text{As}$ barrier layers used in [3] is estimated as $3 \times 10^4 \text{ cm}^{-1}$ [9]. In this case, the total thickness of the barrier layers in [3] was approximately 300 nm, which allowed the authors to pump quantum wells uniformly and efficiently.

5. Conclusions

We have implemented a pulsed semiconductor disk laser based on the $\text{Al}_x\text{Ga}_{1-x}\text{As}/\text{Al}_y\text{Ga}_{1-y}\text{As}$ heterostructure with a built-in Bragg mirror, which emits at a wavelength near 780 nm.

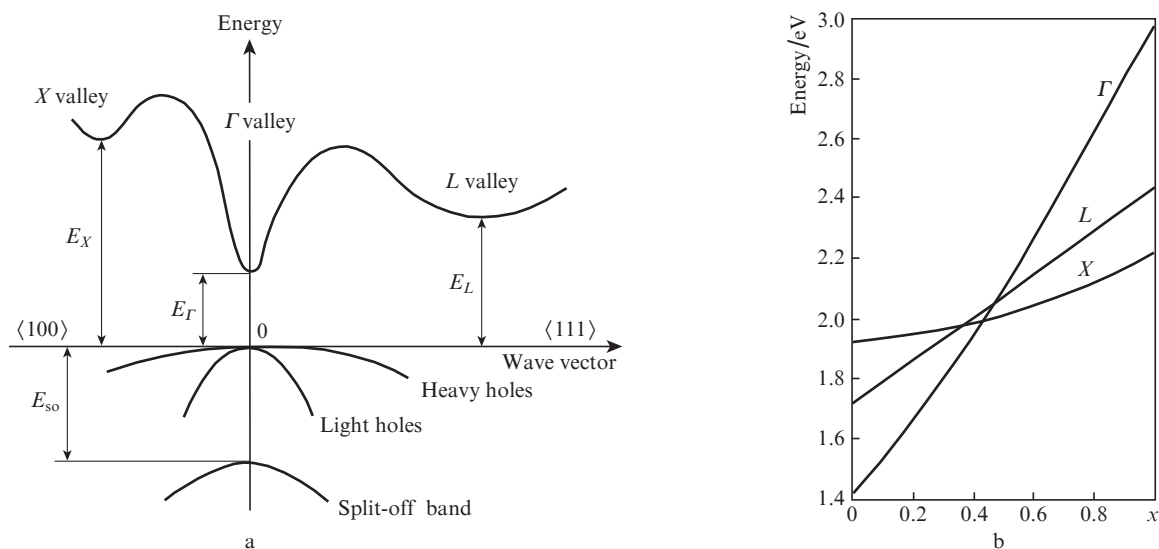


Figure 11. (a) Schematic of the energy band structure of $\text{Al}_x\text{Ga}_{1-x}\text{As}$ at $x < 0.4$ [6] and (b) dependence of the energy gaps E_Γ , E_L , and E_X on the composition of the solid solution [7].

The structure was obtained by the MOCVD method. When pumped by an electron beam, a peak power of 4.4 W was achieved at a slope efficiency of over 10%, while when optically pumped by LD radiation with a wavelength of 450 nm, the power was 0.2 W at a slope efficiency of 2.2%. We explain the lower values of power and efficiency under optical pumping by the inhomogeneous excitation of quantum wells over the depth of the structure due to the high absorption coefficient of pump radiation by the barrier layers. A further increase in the energy characteristics of the laser is possible by increasing the pump wavelength up to 650 nm and optimising the structure parameters.

Acknowledgements. This work was supported by the Russian Foundation for Basic Research (Grant No. 20-32-90022).

References

1. Guina M., Rantamäki A., Härkönen A. *J. Phys. D: Appl. Phys.*, **50**, 383001 (2017).
2. Moriya P.H., Singh Y., Bongs K., Hastie J.E. *Opt. Express*, **28** (11), 15943 (2020).
3. Kahle H., Penttinen J.-P., Phung H.-M., Rajala P., Tukiainen A., Ranta S., Guina M. *Opt. Lett.*, **44** (5), 1146 (2019).
4. Andreev A.Yu., Bagaev T.A., Butaev M.R., Gamov N.A., Zhdanova E.V., Zverev M.M., Kozlovsky V.I., Skasyrsky Ya.K., Yarotskaya I.V. *Quantum Electron.*, **49** (10), 909 (2019) [*Kvantovaya Elektronika*, **49** (10), 909 (2019)].
5. Popov Yu.M. *Trudy FIAN*, **31**, 3 (1965).
6. Goldberg Yu.A. *Handbook Series on Semiconductor Parameters*. Ed. by M. Levinstein, S. Rumyantsev, M. Shur (London: World Scientific, 1999) Vol. 2, pp 1–36.
7. Saxena A.K. *J. Phys. C*, **13** (23), 4323 (1980).
8. Feldmann J., Sattmann R., Peter G., Gobel E.O., Nunnenkamp J., Kuhl J., Hebling J., Ploog K., Cingolani R., Muralidharan R., Dawson P., Foxon C.T. *Surface Sci.*, **229**, 452 (1990).
9. Aspnes D.E., Kelso S.M., Logan R.A., Bhat R. *J. Appl. Phys.*, **60**, 754 (1986).